AMERICAN SOCIETY FOR MICROBIOLOGY | Applied and Environmental Microbiology®

GENETICS AND MOLECULAR BIOLOGY

Species-Specific Quorum Sensing Represses the Chitobiose Utilization Locus in *Vibrio cholerae*

Catherine A. Klancher,[a] Jane D. Newman,[a] Alyssa S. Ball,[a] Julia C. van Kessel,[a] Ankur B. Dalia[a]

[a]Department of Biology, Indiana University, Bloomington, Indiana, USA

ABSTRACT The marine facultative pathogen *Vibrio cholerae* forms complex multicellular communities on the chitinous shells of crustacean zooplankton in its aquatic reservoir. *V. cholerae*-chitin interactions are critical for the growth, evolution, and waterborne transmission of cholera. This is due, in part, to chitin-induced changes in gene expression in this pathogen. Here, we sought to identify factors that influence chitin-induced expression of one locus, the chitobiose utilization operon (*chb*), which is required for the uptake and catabolism of the chitin disaccharide. Through a series of genetic screens, we identified that the master regulator of quorum sensing, HapR, is a direct repressor of the *chb* operon. We also found that the levels of HapR in *V. cholerae* are regulated by the ClpAP protease. Furthermore, we show that the canonical quorum sensing cascade in *V. cholerae* regulates *chb* expression in an HapR-dependent manner. Through this analysis, we found that signaling via the species-specific autoinducer CAI-1, but not the interspecies autoinducer AI-2, influences *chb* expression. This phenomenon of species-specific regulation may enhance the fitness of this pathogen in its environmental niche.

IMPORTANCE In nature, bacteria live in multicellular and multispecies communities. Microbial species can sense the density and composition of their community through chemical cues using a process called quorum sensing (QS). The marine pathogen *Vibrio cholerae* is found in communities on the chitinous shells of crustaceans in its aquatic reservoir. *V. cholerae* interactions with chitin are critical for the survival, evolution, and waterborne transmission of this pathogen. Here, we show that *V. cholerae* uses QS to regulate the expression of one locus required for *V. cholerae*-chitin interactions.

KEYWORDS quorum sensing, cholera, protease

The facultative bacterial pathogen *Vibrio cholerae*, the causative agent of the diarrheal disease cholera, natively resides in the aquatic environment. In this niche, *V. cholerae* forms multicellular communities on biotic and abiotic chitinous surfaces, like the shells of crustaceans or marine snow (1, 2). Chitin is a polysaccharide made up of β-1,4-linked *N*-acetylglucosamine (GlcNAc) and serves as a major nutrient source for *V. cholerae* in the marine environment (1, 3, 4). The ability of *V. cholerae* to form chitin biofilms is critical for the waterborne transmission of cholera (5, 6). As chitin is the most abundant biopolymer in the ocean, the ability of *Vibrio* species to break down and utilize this highly insoluble polysaccharide also serves an important role in global nitrogen and carbon recycling (1, 4).

When *V. cholerae* is associated with a chitinous surface, chitin induces the expression of a subset of genes in *V. cholerae*. The genes induced by chitin include those required for chitin degradation, uptake, and catabolism (termed the chitin utilization program), as well as the genes required for natural transformation (7, 8). Transcriptional responses resulting from *Vibrio*-chitin interactions are highly regulated. One major chitin-responsive regulator is the orphan hybrid sensor kinase ChiS (7, 9). ChiS senses chitin

Citation Klancher CA, Newman JD, Ball AS, van Kessel JC, Dalia AB. 2020. Species-specific quorum sensing represses the chitobiose utilization locus in *Vibrio cholerae*. Appl Environ Microbiol 86:e00915-20. https://doi.org/10.1128/AEM.00915-20.

Editor Eric V. Stabb, University of Illinois at Chicago

Address correspondence to Ankur B. Dalia, ankdalia@indiana.edu.

Received 16 April 2020
Accepted 4 July 2020
Accepted manuscript posted online 10 July 2020
Published 1 September 2020

indirectly through the periplasmic chitin binding protein (CBP) (9, 10). In the absence of chitin, CBP represses ChiS through interactions with its periplasmic domain (9, 10). In the presence of chitin, the CBP-chitin complex stimulates ChiS activity (9, 10). Thus, in the presence of chitin, ChiS is active and can facilitate expression of the chitin utilization program. Alternatively, ChiS can be genetically activated in the absence of chitin by deleting *cbp* (10, 11).

In the marine environment, *V. cholerae* not only senses chitin to modulate gene expression but also the presence of other bacteria through a process termed "quorum sensing" (QS) (12). This is a process by which bacteria indirectly sense other microbes in their community via small diffusible molecules called autoinducers (AIs). AIs are sensed by cognate sensor proteins. *V. cholerae* has four AI sensors, although the autoinducer molecules that serve as inducing cues are only known for two of them (13). AI sensing allows for cell-density-specific gene expression programs, which regulate "group" or "individual" behaviors (14). *V. cholerae* senses both chitin and AIs to regulate natural transformation on chitinous surfaces (15). Though a link between chitin utilization and quorum sensing has previously been suggested, it has not been directly studied (16).

To investigate regulation of the chitin utilization program in *V. cholerae*, most studies employ the chitobiose utilization operon (*chb*) (10, 11, 17, 18). The *chb* operon encodes the genes required for uptake and catabolism of the chitin disaccharide chitobiose and is highly induced in the presence of chitin oligosaccharides (7). Several mechanisms of *chb* regulation have already been identified. ChiS is the master regulator of the chitin utilization program in *V. cholerae*, and we have recently shown that this protein is a direct transcriptional activator required for induction of the *chb* locus (9, 10). Previous work has shown that carbon catabolite repression (CCR) can also play a role in regulating chitin responsive phenotypes, including ChiS-dependent induction of *chb* and natural transformation (18, 19). In addition, our group has previously found that the cell division licensing factor SlmA plays an essential role in activating *chb* expression (11). Tight regulation via these diverse signaling systems may act to ensure that the chitin utilization program is only expressed under conditions in which it will provide a competitive advantage.

Here, we sought to identify additional regulators of *chb*. Through a number of genetic screens and complementary molecular methods, we show that quorum sensing is an additional regulatory system that tunes expression of a chitin utilization locus in *V. cholerae*.

RESULTS

ClpA is identified in an unbiased screen for activators of P_{chb}. To identify additional genes required for activation of the *chb* locus, we conducted a transposon mutant screen. This was carried out in a strain containing a chromosomally integrated P_{chb}-*lacZ* transcriptional reporter. As shown previously, induction of P_{chb} is dependent on the activity of the master regulator ChiS (7, 10, 11). In the absence of chitin, ChiS activity is repressed by CBP. In the presence of chitin, CBP repression of ChiS is relieved, which allows for ChiS-dependent activation of P_{chb}. In addition to being induced by chitin, ChiS can be activated genetically in the absence of chitin by deleting *cbp* (10, 11). As chitin oligomers are prohibitively expensive, a Δ*cbp* mutation was used to induce ChiS-dependent P_{chb}-*lacZ* expression in our genetic screen exactly as previously described (11). So, the starting genotype for our screen was a strain containing P_{chb}-*lacZ* and a Δ*cbp* mutation. This strain formed blue colonies on 5-bromo-4-chloro-3-indolyl-β-D-galactopyranoside (X-Gal)-containing plates, and we screened for white colonies to identify putative activators that contribute to P_{chb} induction.

Of approximately 60,000 transposon mutants visually screened for loss of P_{chb}-*lacZ* expression, one gene identified was *clpA* (2 unique transposon insertions). Other hits identified in this screen are listed in Table S1 in the supplemental material. To study the effect of *clpA* on P_{chb} activity moving forward, we utilized a previously described chromosomally integrated P_{chb}-green fluorescent protein (GFP) reporter (10, 11). Using

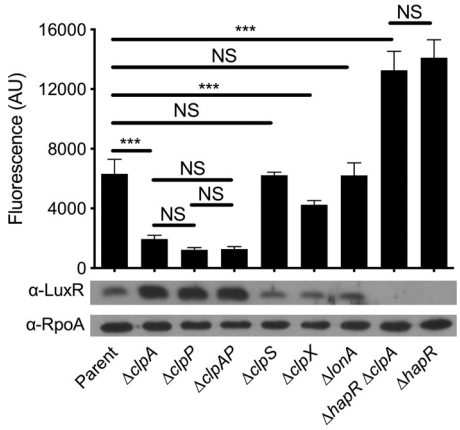

FIG 1 HapR is a repressor of P_{chb} that is degraded by the ClpAP protease. Expression of a P_{chb}-GFP reporter and HapR protein levels were determined in the indicated mutant strains. The parent strain contained a P_{chb}-GFP reporter and a Δ*cbp* mutation. A representative Western blot is shown below bars to indicate the protein levels for HapR and RpoA (a loading control) in the corresponding strains. An antibody against LuxR, which has 72% identity and 86% similarity to HapR, is cross-reactive with HapR and so was used to detect HapR protein levels. Fluorescence of cultures was determined on a plate reader from at least six independent biological replicates and is shown as the mean ± standard deviation (SD). Statistical comparisons were made by one-way ANOVA with Tukey's posttest. NS, not significant. ***, $P < 0.001$.

this reporter, we found that a Δ*clpA* mutation resulted in an ~3-fold decrease in P_{chb} expression relative to the parent (Fig. 1). Importantly, complementation of this strain with an ectopic copy of *clpA* in *trans* restored P_{chb} expression to parent levels (see Fig. S1 in the supplemental material). ClpA is a AAA+ unfoldase that recognizes protein substrates, unfolds them, and feeds them into the ClpP protease where they are degraded (20). If ClpA was exhibiting its effect on P_{chb} expression as a part of the ClpAP machine, we hypothesized that a Δ*clpP* mutation should phenocopy a Δ*clpA* mutation. Indeed, Δ*clpP* and Δ*clpP* Δ*clpA* strains phenocopied a Δ*clpA* mutant for P_{chb} expression (Fig. 1). These results suggest that loss of the ClpAP protease decreases P_{chb} expression. As ClpAP degrades proteins, we hypothesized that ClpAP may indirectly promote activation of P_{chb} by degrading a repressor of the *chb* locus.

HapR is a repressor of P_{chb} that is degraded by ClpAP. To identify a putative repressor of P_{chb} that is targeted by ClpAP for degradation, we conducted a counterscreen using the P_{chb}-*lacZ* reporter. For the Δ*clpA* strain counterscreen, the parent strain had both Δ*cbp* and Δ*clpA* mutations. This mutant is white on X-Gal plates because P_{chb}-*lacZ* is poorly expressed; inactivation of the putative repressor in this strain should result in restoration of P_{chb}-*lacZ* expression and yield a blue colony phenotype. In the Δ*clpA* strain counterscreen, we visually screened approximately 30,000 transposon mutants for reactivation of P_{chb}-*lacZ* expression and identified *hapR* (9 unique transposon insertions). Other hits identified in this screen are listed in Table S1. A Δ*hapR* mutation restored P_{chb} expression in the Δ*clpA* mutant background (Fig. 1). In fact, a Δ*hapR* mutation allowed for higher P_{chb} expression than that of the parent strain. This suggests that HapR represses P_{chb} expression when ClpAP is intact and that ClpAP does not degrade the entire pool of HapR in the cell (Fig. 1). Importantly, the level of P_{chb} expression observed in the Δ*hapR* Δ*clpA* mutant phenocopied the Δ*hapR* strain (Fig. 1). This epistasis between *clpA* and *hapR* suggests that they are involved in the same pathway for regulating P_{chb} expression. In addition, complementation of the Δ*hapR* strain with an ectopic copy of *hapR* in *trans* decreased P_{chb} expression almost to the level in the parent (see Fig. S1). Further, complementation of the Δ*hapR* Δ*clpA* strain with *hapR* in *trans* brought P_{chb} expression down to the level observed in the Δ*clpA* parent (Fig. S1).

We hypothesized that the reason P_{chb} expression was decreased in Δ*clpAP* mutants was due to increased HapR protein levels. Western blotting in these backgrounds

revealed that HapR levels were, indeed, increased in strains containing mutations to *clpA* and/or *clpP* (Fig. 1). ClpAP-dependent degradation of HapR is not unique to *V. cholerae* but has previously been observed in *Vibrio vulnificus* where ClpAP degrades the HapR homolog SmcR (21). In addition to the ClpAP machine, it was shown that the Lon protease also plays a role in SmcR degradation. So, we next sought to investigate the role of other protease machines on induction of P_{chb} and HapR protein levels. Mutations to other Clp components (the ClpS adaptor protein or the ClpX unfoldase) did not have a marked impact on HapR protein levels. Also, a Δ*clpS* mutation did not affect P_{chb} expression levels, while a Δ*clpX* mutation slightly decreased P_{chb} expression (Fig. 1). Because HapR expression was not affected by the Δ*clpX* mutation, the observed decrease in P_{chb} expression may be attributed to a pleiotropic effect (i.e., an effect of *clpX* that is independent of HapR-dependent P_{chb} repression). In contrast to the effect of the Lon protease on SmcR levels in *V. vulnificus*, we did not observe an impact of the Δ*lonA* mutation on HapR levels in *V. cholerae*; the Δ*lonA* mutation, correspondingly, did not affect P_{chb} expression (Fig. 1). Together, these results establish that HapR is a repressor of P_{chb} and that HapR levels are controlled specifically by the ClpAP protease in *V. cholerae*.

HapR-mediated repression of P_{chb} occurs on chitinous surfaces. Thus far, we have studied P_{chb} regulation using a Δ*cbp* mutation to induce ChiS activity. Natural induction of this locus, however, occurs in the presence of chitin oligosaccharides. So, we next wanted to test whether the repression of P_{chb} by HapR was observed in a more physiologically relevant setting. To test this, we cultured *V. cholerae* strains with CBP intact, a P_{chb}-mCherry reporter, and a construct that constitutively expresses GFP (P_{const2}-GFP) on chitin beads (Fig. 2A). The P_{const2}-GFP construct (derived from the insulated *proD* promoter [22]) served as an internal control for noise in gene expression and was used to normalize P_{chb}-mCherry expression in single cells (see Materials and Methods for details).

When cells were cultured on chitin beads, both the parent strain and the Δ*hapR* strain exhibited a bimodal distribution of P_{chb} expression (Fig. 2A to C). There were at least two possible explanations for the observed bimodality in P_{chb} gene expression in this experiment as follows: (i) the signaling pathway that leads to activation of *chb* has switch-like behavior that results in a population that exhibits bimodality in *chb* expression, or (ii) the environment during growth on chitin beads is heterogeneous and only some cells within the population have access to the chitin oligosaccharides necessary for activation of *chb*. Those cells that do not have access to chitin do not activate P_{chb} expression (P_{chb} off), while those that do have access to chitin do induce P_{chb} expression (P_{chb} on). To differentiate between these two possibilities, we induced expression of P_{chb} using the native inducer, chitin oligosaccharides, or genetically by deleting *cbp*. If the signaling circuit responsible for P_{chb} activation has switch-like behavior, we would predict that bimodality in gene expression would be maintained in both of these conditions; however, if bimodality is the result of heterogeneous access to chitin oligosaccharides when cells are cultured on chitin beads, we would expect bimodality to be lost. When P_{chb} was induced by chitin oligosaccharides or via deletion of *cbp*, all cells in the population are uniformly "P_{chb} on" (Fig. 2D and F), and the population becomes unimodal (Fig. 2E and G). Thus, these results showed that only the "P_{chb} on" cells have access to chitin oligosaccharides when grown on chitin beads. These results are consistent with chitin induction of natural transformation on chitin beads, where cells display bimodality in gene expression that is also likely due to heterogeneous access to inducing chitin oligosaccharides (23).

Next, we tested whether HapR influenced activation of P_{chb} on chitin beads by just assessing the expression level among "P_{chb} on" cells. As observed in bulk populations, the Δ*hapR* strain exhibited an ~1.7-fold increase in P_{chb} expression when cultured on chitin beads (Fig. 2C) and an ~2.5-fold increase when cultured with chitin oligosaccharides (Fig. 2E). These values were consistent with the ~2-fold increase in P_{chb} expression observed in single cells when the population was induced via deletion of

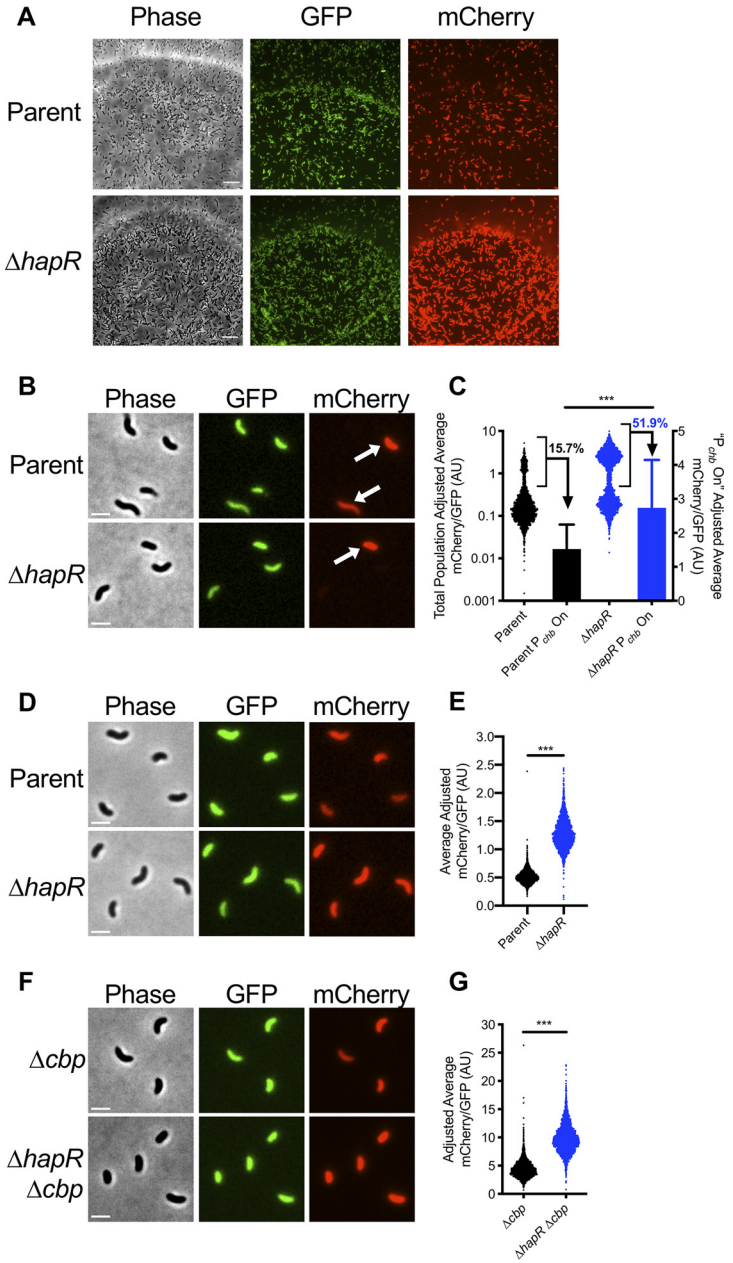

FIG 2 HapR-mediated repression of P_{chb} occurs on chitinous surfaces. (A) Representative images of the indicated *V. cholerae* strains grown on chitin beads. The parent strain background contains both a P_{chb}-mCherry reporter and a P_{const2}-GFP construct, which exhibits constitutive GFP expression. Scale bar = 10 μm. (B and C) P_{chb} expression in the indicated *V. cholerae cbp*$^+$ strains grown on chitin beads. (B) Representative images of cells that were vortexed off chitin beads. Arrows demarcate cells where P_{chb} expression is induced ("P_{chb} on" cells). Scale bar = 2 μm. (C) Scatterplot and bar graph showing the relative expression of the P_{chb}-mCherry reporter in cells cultured on chitin beads. Scatterplots (left *y* axis) represent the entire population, whereas the bars (right *y* axis) represent only the P_{chb} on cells (bracketed in black on scatterplots). The percentage of cells in the P_{chb} on population is indicated. n = 2,120 for parent; n = 2,191 for Δ*hapR* strain; n = 333 for parent P_{chb} on; n = 1,139 for Δ*hapR* strain P_{chb} on. Data shown are from two independent biological replicates. (D and E) P_{chb} expression of the indicated *V. cholerae* strains where P_{chb} expression is induced by chitin oligosaccharides. (D) Representative images of cells grown with chitin oligosaccharides. Scale bar = 2 μm. (E) Scatterplot showing the relative expression of a P_{chb}-mCherry reporter in the indicated *V. cholerae* strains. n = 2,735 for parent; n = 2,384 for Δ*hapR* strain. Data shown are from two independent biological replicates. (F and G) P_{chb} expression of the indicated *V. cholerae* strains where P_{chb} expression is induced via deletion of *cbp*. (F) Representative images of cells grown in the absence of chitin. Scale bar = 2 μm. (G) Scatterplot showing the relative expression of a P_{chb}-mCherry reporter in the indicated *V. cholerae* strains. n = 2,407 for Δ*cbp* strain; n = 2,313 for Δ*hapR* Δ*cbp* strain. Data shown are from two independent biological replicates. Statistical comparisons in panels C, E, and G were made using Student's *t* test. ***, $P < 0.001$.

cbp (Fig. 2G). Finally, native *chb* transcripts (measured via reverse transcription-quantitative PCR [qRT-PCR]) were also induced ~2-fold higher in a Δ*hapR* mutant compared to that of the parent when strains were induced with chitin oligosaccharides (see Fig. S2 in the supplemental material). Together, these results indicate that HapR is a bona fide repressor of P_{chb} under physiologically relevant inducing conditions.

HapR repression of P_{chb} is conserved in other *V. cholerae* El Tor isolates. Previously, it was suggested that HapR was an activator of P_{chb} expression in the *V. cholerae* El Tor isolate A1552 (16). Specifically, the authors showed that deletion of *hapR* resulted in a decrease in P_{chb} expression when cells were cultured on chitin flakes. In the present study, we use the *V. cholerae* El Tor isolate E7946 to study P_{chb} regulation. To assess if HapR exhibits different effects on P_{chb} expression depending on the strain background, we assessed expression of a P_{chb}-mCherry reporter in *hapR*$^+$ and Δ*hapR* derivatives of both E7946 and A1552. Consistent with our previous results, we observed that P_{chb} expression is elevated ~2-fold in the Δ*hapR* derivative of both strain backgrounds when induced with chitin oligosaccharides or via deletion of *cbp*, which is consistent with HapR acting as a repressor of this locus (see Fig. S3 in the supplemental material). It is unclear what explains the discrepancy between our findings and those that were previously reported; however, these data suggest that they cannot be attributed to differences between strain backgrounds.

Deletion of HapR does not confer a growth advantage during growth on chitobiose. Our data indicate that in the absence of HapR, P_{chb} expression is elevated. The *chb* locus encodes the genes required for uptake and degradation of the chitin disaccharide, chitobiose. Thus, we wanted to assess if the increased expression of P_{chb} confers a fitness advantage to Δ*hapR* mutant cells during growth on chitobiose. To test this, we conducted competitive growth assays with a 1:1 mixture of a parent and a Δ*hapR* mutant strain on minimal medium with chitobiose as the sole carbon source. We hypothesized that if the Δ*hapR* mutant had a competitive growth advantage due to increased expression of *chb*, then it should outcompete the parent strain in this assay. Even after ~48 generations of growth on chitobiose, however, we did not observe a competitive advantage for the Δ*hapR* mutant (see Fig. S4 in the supplemental material). HapR is a global regulator that controls the expression of dozens of genes (24). Thus, even though a Δ*hapR* mutant has increased P_{chb} expression, there may be negative pleiotropic effects associated with the Δ*hapR* mutation that masks any competitive advantage of derepression of P_{chb} in this mutant during growth on chitobiose.

HapR binds P_{chb} *in vitro* and *in vivo*. Thus far, our data suggest that HapR is a repressor of P_{chb}, but it does not distinguish whether HapR is a direct or indirect regulator of this locus. To assess if HapR could be regulating P_{chb} directly, we used an *in silico* approach to identify putative HapR binding sites (BSs) in P_{chb} based on consensus binding sequences generated for the HapR homologs LuxR (from *Vibrio harveyi*) and SmcR (from *V. vulnificus*) via chromatin immunoprecipitation sequencing (ChIP-seq) (25, 26). Using the Motif Alignment and Search Tool (MAST) in the Multiple Em for Motif Elicitation (MEME) suite (27), we identified two potential HapR binding sites in P_{chb} (Fig. 3A). Interestingly, these binding sites overlap with other elements in the *chb* promoter required for transcriptional activation. HapR BS 1 overlaps with the SlmA binding site, which is a critical activator of P_{chb} expression (11). HapR BS 2 overlaps with the −35 signal, which is required for RNA polymerase to bind to the promoter and initiate transcription. This sequence analysis suggests that the repressive effect of HapR may be due to HapR binding directly antagonizing SlmA and/or RNA polymerase (RNAP) at this locus.

We next sought to determine whether HapR could directly bind to P_{chb} using both *in vitro* and *in vivo* approaches. First, we tested whether HapR could bind to P_{chb} *in vitro* using electrophoretic mobility shift assays (EMSAs). Consistent with the presence of two HapR binding sites in P_{chb}, we observed two shifts by EMSA when using a DNA probe of the *chb* promoter (Fig. 3B). HapR does not regulate the ClpP promoter and thus did not bind P_{clpP} (Fig. 3B), which is consistent with previous studies (28). EMSAs were also done using 32-bp probes that encompassed each putative HapR BS (probe sequences

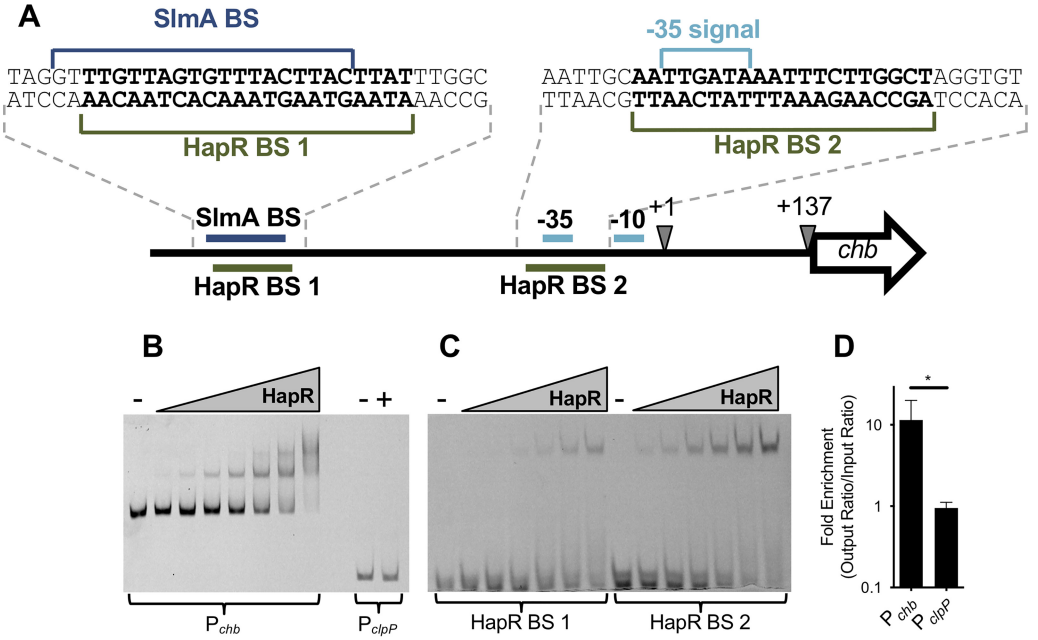

FIG 3 HapR binds P_{chb} *in vitro* and *in vivo*. (A) Promoter map of P_{chb} highlighting putative HapR binding sites (BSs). Other sites required for P_{chb} activation (the SlmA BS and the −35 and −10 signals) are highlighted. The exact sequences of the region containing the HapR BSs (bolded), the SlmA BS, and the −35 signal are shown. The transcriptional start site (+1) and the translational start site (+137) are also shown. (B) A representative EMSA using HapR and Cy5-labeled DNA probes of the indicated promoters. The P_{chb} probe was incubated with (from left to right) 0 nM (−), 12.5 nM, 25 nM, 50 nM, 100 nM, 200 nM, 400 nM, or 800 nM purified HapR. The P_{clpP} probe was incubated with 0 nM (−) or 800 nM HapR (+). (C) A representative EMSA using HapR and 32-bp Cy5-labeled probes encompassing each of the putative HapR binding sites within the *chb* promoter (exact probe sequences are shown in panel A). The 32-bp probes were incubated with (from left to right) 0 nM (−), 100 nM, 200 nM, 400 nM, 800 nM, 1.6 μM, or 3.2 μM purified HapR. (D) ChIP-qPCR assays showing enrichment of the indicated promoters relative to *rpoB*, a reference locus that HapR does not bind to. Data are from five independent biological replicates and are shown as the mean ± SD. Statistical comparisons were made by Student's *t* test. *, $P = 0.0240$.

can be found in Fig. 3A). We observed that HapR was able to bind to both probes, suggesting that HapR binds to both HapR BS 1 and HapR BS 2 (Fig. 3C). Next, we wanted to assess if HapR bound to P_{chb} *in vivo* via ChIP assays under physiologically relevant conditions. To that end, we first generated a FLAG-HapR strain that was functional for regulating P_{chb} expression (see Fig. S5 in the supplemental material). Using this strain in ChIP-quantitative PCR (qPCR) assays, we found that P_{chb} was, indeed, bound by HapR *in vivo*, while the negative control P_{clpP} locus was not bound by HapR (Fig. 3D). Together, these data demonstrate that HapR binds to P_{chb}, which suggests that it is a direct repressor of this locus.

Quorum sensing regulates expression of P_{chb} through the cholera-specific autoinducer CAI-1. HapR is the master regulator of quorum sensing (QS) in *V. cholerae* and is highly expressed at high cell density (HCD) (29). Thus far, we have established that HapR is a repressor of P_{chb} expression. Next, we wanted to probe the role of QS in regulating P_{chb}. To that end, we sought to test the effect of mutations in genes upstream of HapR in the *V. cholerae* QS cascade on P_{chb} induction and HapR protein levels.

QS in *Vibrio* species is controlled by autoinducer-responsive sensor proteins that indirectly modulate phosphorylation of the response regulator LuxO, which in turn indirectly regulates production of HapR (14). When autoinducer concentrations are low (i.e., at low cell density [LCD]), multiple histidine kinase sensors act as kinases (30–32). This results in high levels of phosphorylated LuxO, which prevents HapR production (see Fig. S6A in the supplemental material) (33). By contrast, at high autoinducer concentrations (i.e., at HCD), the sensors act as phosphatases, which ultimately leads to dephosphorylation of LuxO and allows for HapR production (Fig. S6B) (14, 34).

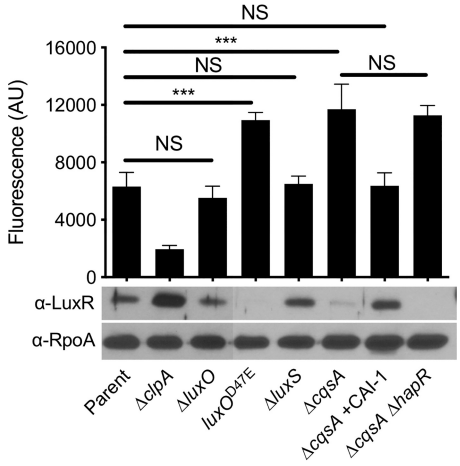

FIG 4 Quorum sensing regulates expression of P_{chb} through the cholera-specific autoinducer CAI-1. Expression of a P_{chb}-GFP reporter and HapR protein levels were determined in the indicated strains. The parent strain contains a P_{chb}-GFP reporter and a Δ*cbp* mutation. A representative Western blot is shown below the bars to indicate the protein levels for HapR and RpoA (a loading control) in the corresponding strains. An antibody against LuxR, which has 72% identity and 86% similarity to HapR, is cross-reactive with HapR and so was used to detect HapR protein levels. Statistical comparisons were made by one-way ANOVA with Tukey's posttest. NS, not significant. ***, $P < 0.001$. The P_{chb}-GFP fluorescence data for the "parent" and "Δ*clpA*" strains are identical to the data presented in Fig. 1 and were included here to ease comparisons.

First, we assessed the impact of HCD on P_{chb} induction and HapR levels by deleting *luxO*, which genetically locks cells in an HCD state. Induction of the parent strain is tested under HCD conditions; thus, as expected, HapR levels were similar between the parent and the Δ*luxO* mutant; accordingly, expression of P_{chb} was also similar between the parent and Δ*luxO* mutant (Fig. 4). Next, we tested the effect of LCD on P_{chb} and HapR expression by generating a $luxO^{D47E}$ (D-to-E change at position 47 encoded by *luxO*) mutant, which mimics phosphorylated LuxO and genetically locks cells in an LCD state. In this strain, we saw that P_{chb} expression increased and was correlated with a decrease in HapR protein levels (Fig. 4). Together, these data suggest that HapR repression of P_{chb} is mediated through the canonical QS circuit.

Next, we wanted to move further upstream in the QS regulatory cascade to address whether distinct autoinducers differentially affected expression of P_{chb} and HapR. There are four parallel histidine kinase sensors that coordinate QS-dependent control of HapR expression (13); however, the autoinducer signal is only known for two of these systems. The sensor LuxPQ is responsive to the interspecies autoinducer AI-2, and the sensor CqsS is responsive to the *V. cholerae*-specific autoinducer CAI-1 (Fig. S6) (35). To assess the role of each autoinducer in regulation of P_{chb}, we made mutations to the synthase genes responsible for production of each autoinducer. LuxS makes AI-2 (36) and CqsA makes CAI-1 (35) (Fig. S6). In a strain that no longer produces AI-2 (Δ*luxS* strain), expression of P_{chb} was similar to that observed in the parent, and HapR levels remained similar in these two strains (Fig. 4). By contrast, a strain that is unable to produce CAI-1 (Δ*cqsA* strain) had increased expression of P_{chb}, likely due to the low level of HapR produced (Fig. 4). The observed decrease in P_{chb} expression in the Δ*cqsA* strain background was, indeed, due to a lack of CAI-1 production, as exogenously adding back synthetic CAI-1 restored HapR levels and repression of P_{chb} to the parent level (Fig. 4). In addition, a strain that does not make CAI-1 induced P_{chb} to the same level as that of a strain that does not produce both CAI-1 or HapR (Fig. 4). This epistasis indicates that CAI-1 production and HapR are involved in the same regulatory pathway for modulating expression of P_{chb}. These data support previous results, which indicate that CqsS signaling plays a dominant role in regulating HapR (23, 35, 37, 38). Together, these results indicate that P_{chb} expression is strongly influenced by QS signaling mediated by the *V. cholerae*-specific autoinducer CAI-1 and less via the interspecies autoinducer AI-2.

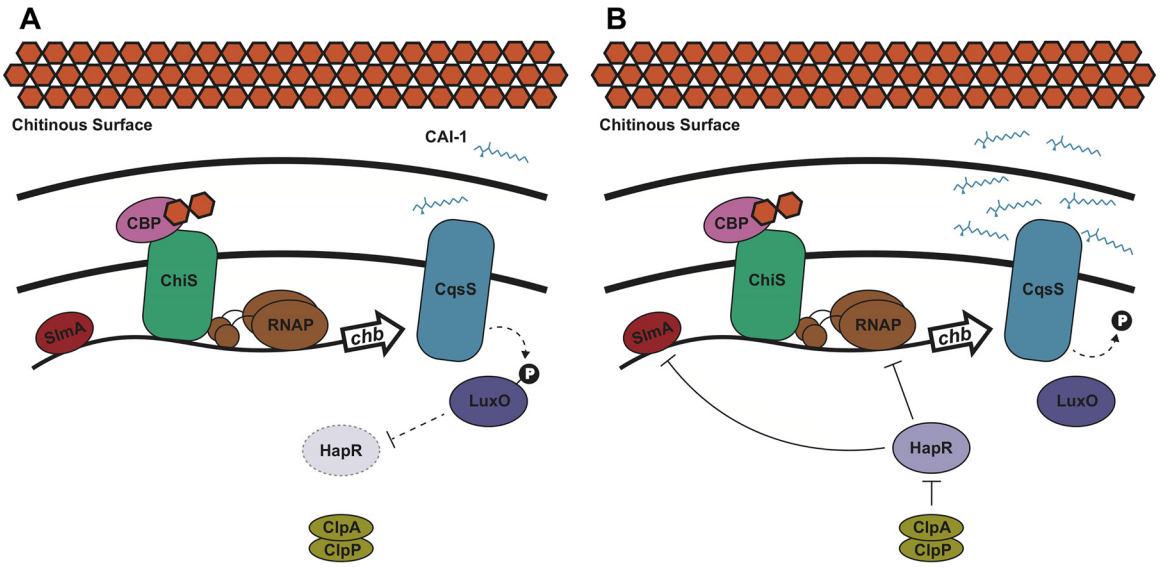

FIG 5 Model of quorum sensing regulation of chitobiose utilization genes in *V. cholerae*. When *V. cholerae* grows on a chitinous surface, the periplasmic chitin binding protein (CBP) binds to chitin oligosaccharides. This derepresses ChiS, which can then activate expression of the chitobiose utilization operon (*chb*) through recruitment of RNA polymerase (RNAP) (10). Binding of SlmA to P_{chb} is also required for transcriptional activation (11). (A) At low CAI-1 concentrations, the CqsS sensor indirectly (dashed line) promotes LuxO phosphorylation, which indirectly blocks HapR expression. In this state, P_{chb} is maximally expressed. (B) At high CAI-1 concentrations, the CqsS sensor indirectly dephosphorylates LuxO, which results in indirect activation of HapR expression. HapR then exerts a repressive effect on P_{chb} by decreasing expression of this locus ~2-fold in the presence of the ClpAP protease machine. If HapR is not degraded by ClpAP, its repressive effect can result in an ~7-fold decrease in P_{chb} expression. The mechanism of HapR repression may be through occluding binding of SlmA or RNAP to P_{chb}.

DISCUSSION

Here, we show that HapR acts as a repressor of chitobiose utilization genes in *V. cholerae*. When this organism forms communities on a chitinous surface, chitin induces expression of P_{chb} through activation of the chitin sensor ChiS (Fig. 5). *V. cholerae* then modulates P_{chb} expression depending on the presence of other *V. cholerae* cells, which it senses via the *V. cholerae*-specific autoinducer CAI-1. At low CAI-1 concentrations, P_{chb} expression is high because the repressor HapR is produced at a low level (Fig. 5A). At high CAI-1 concentrations, HapR is produced at higher levels and can repress P_{chb} expression (Fig. 5B). As the HapR binding sites in P_{chb} overlap with the SlmA binding site and the −35 signal, it is possible that HapR competes with these activators for binding at P_{chb}. Thus, HapR-mediated repression may occur through antagonism of the binding activity of SlmA and/or RNAP at P_{chb}.

When HapR is produced, it gets proteolyzed by the ClpAP machine (Fig. 5B). While the dynamic range of HapR-dependent P_{chb} repression is only ~2-fold when ClpAP is intact, the dynamic range of repression increases to ~7-fold in the absence of ClpAP. Thus, it is tempting to speculate that regulation of ClpAP may modulate P_{chb} expression under some conditions. Currently, however, little is known about the regulation of ClpAP in *V. cholerae*. ClpAP is induced during heat shock in *V. vulnificus* (21). Also, in *Escherichia coli*, ClpP expression is induced during heat shock (39–41). Thus, it is believed that the ClpP protease plays a role in the heat shock response. In *Bacillus subtilis*, ClpP is upregulated under various stress conditions, suggesting that this protease may also be induced by a general stress response (42). Thus, one possibility is that stress-dependent regulation of ClpAP indirectly regulates P_{chb}. It has also been hypothesized that *V. cholerae* makes use of proteolysis machines to rapidly respond to changes in their environment; namely, the transition from the human gut to the aquatic environment after infection (43). ClpAP acting as an activator of P_{chb} may be a way for cells to rapidly induce expression of a locus that is not important in the human gut but is useful for survival in its aquatic reservoir. Consistent with this idea, *chb* is induced late

in infection, suggesting that this is a critical locus for preparing to reenter the aquatic environment after infection of a host (44).

The mechanisms underlying distinct responses to AI-2 or CAI-1 remain a topic of interest in QS. It has been shown that the CAI-1 sensor CqsS plays a dominant role over LuxPQ in modulating HapR levels. Thus, it remains possible that the presence of CAI-1 allows for more robust regulation of HapR-regulated genes. CAI-1 has been shown to be critical for expression of the virulence factor *hapA* (38), natural transformation (15), and for repressing chitobiose utilization as shown in this study. HapA is a protease that has been implicated in mediating *V. cholerae* detachment from host epithelial cells, thereby promoting dissemination of cells back into the aquatic environment (45, 46); natural transformation and chitin utilization aid in *V. cholerae* fitness in the marine environment. By contrast, expression of *tcpA*, a protein that contributes to *V. cholerae* pathogenesis in the human gut, was shown to be primarily regulated by AI-2 (37). It is tempting to speculate that CAI-1 controls *V. cholerae* behaviors important for marine survival, whereas AI-2 controls behaviors involved in infection. It has been hypothesized that sensing both of these autoinducers plays a critical role in biofilm dispersal and that only when both are sensed are *V. cholerae* cells induced to leave a surface (i.e., QS works as a coincidence detector for both signals) (37). Thus, signaling via distinct autoinducers may allow *V. cholerae* to modulate responses depending on the context of the environment that they inhabit.

The data that we present here suggests that at HCD, *V. cholerae* dampens its expression of a chitin utilization locus. Below, we speculate on a few reasons why this regulation may be advantageous. Chitin polymers in the shells of crustacean zooplankton are long-chain polysaccharides in a crystalline insoluble lattice. In order to be used as a nutrient source, the long-chain chitin must be broken down into smaller, soluble chitin oligosaccharides. *V. cholerae* secretes chitinases that enzymatically degrade insoluble chitin into soluble chitin oligosaccharides for uptake and catabolism. The production and secretion of chitinases is an energetically costly process; thus, liberated chitin is a valuable "public good" in the context of a chitin biofilm (47). So, it is possible that QS regulation of chitin utilization allows *V. cholerae* to modulate chitin uptake based on the composition of its microbial community. When the level of *V. cholerae* cells (and the corresponding concentration of cholera-specific autoinducer CAI-1) in the community is high, chitin uptake may decrease among individual cells within the population in an effort to "share" liberated chitin oligosaccharides. By contrast, when the level of *V. cholerae* in the community is low, sensing of only the interspecies signal AI-2 (which is produced by many bacterial species) does not suppress chitin uptake and utilization, thus, allowing the *V. cholerae* within this population to maximally compete for liberated chitin oligosaccharides.

Another possibility is that this regulation allows *V. cholerae* to control its production of toxic metabolites. In a previous study, it was shown that cells in an HCD state alter their metabolic flux to produce neutral by-products as opposed to organic acids when grown in LB supplemented with a fermentable sugar like glucose (48). This regulation allows for a more stable community; by contrast, cells locked in an LCD state will excrete harmful metabolic by-products, which leads to the demise of the community (48). It has been shown that *V. cholerae* excretes ammonium as a potentially toxic by-product when grown on chitin (16). Also, because chitin oligosaccharides likely feed into glycolysis, it is possible that catabolism of chitin results in the production of potentially toxic organic acids. Thus, repressing chitin uptake and utilization may also help slow the rate of metabolism to prevent the accumulation of toxic intermediates in a dense community setting.

MATERIALS AND METHODS

Bacterial strains and culture conditions. *V. cholerae* strains were routinely grown at 30°C in LB medium and on LB agar supplemented when necessary with carbenicillin (20 μg/ml or 50 μg/ml), kanamycin (50 μg/ml), spectinomycin (200 μg/ml), trimethoprim (10 μg/ml), and/or chloramphenicol (2 μg/ml). Strains were grown in defined artificial salt water (DASW) medium for microscopy (see below

for details), Instant Ocean for generating mutant strains (see below for details), or M9 minimal medium for competition experiments (see below for details).

Transposon mutagenesis. Transposon mutant libraries were generated with a Carb^r mini-Tn*10* transposon exactly as previously described (49). Briefly, the transposon mutagenesis plasmid pDL1086 was first mated into parent strains containing chromosomally integrated P_{chb}-*lacZ* and a Δ*cbp* mutation (activator screen) or Δ*clpA* Δ*cbp* mutations (Δ*clpA* strain counterscreen). The parent strains also carried a chromosomally integrated P_{chb}-mCherry reporter at an ectopic site to ensure that candidate transposon mutants affected expression of P_{chb} and did not simply disrupt the P_{chb}-*lacZ* reporter. The activator screen parent also carried an additional copy of ChiS at an ectopic site, which prevented transposon hits in this known regulator of P_{chb}. Transposition was induced by plating cultures on LB agar supplemented with 50 μg/ml carbenicillin (Carb) at 42°C. To screen colonies, plates also contained 40 μg/ml X-Gal and 5 mM isopropyl-β-D-thiogalactopyranoside (IPTG). IPTG was added to competitively inhibit the basal activity of the P_{chb}-*lacZ* reporter.

The sequences of transposon-genomic junctions in transposon mutants were determined by inverse PCR followed by Sanger sequencing. Briefly, genomic DNA was purified from mutants of interest and digested with the FatI restriction enzyme per the manufacturer's instructions (NEB). Digested genomic DNAs were then incubated with T4 DNA ligase per manufacturer's instructions (NEB) to generate self-ligated circles. The transposon-genomic junction was then amplified by PCR using the primers specified in Table 1 and subsequently Sanger sequenced (Eurofins Genomics).

Generating mutant strains. *V. cholerae* E7946 served as the parent for all strains generated in this study, except for those used in Fig. S3 in the supplemental material where we compare E7946 to A1552 (50, 51). Mutant constructs were generated by splicing by overlap extension PCR (SOE PCR) exactly as previously described with the primers indicated in Table 1 (52). PCRs were performed to generate up (F1/R1), middle, and down (F2/R2) arms. Up and down arms were designed to have 3-kb arms of homology to the genome at the site targeted for mutagenesis. All three arms were then mixed and used as a template for SOE PCRs with the F1 and R2 primers to generate the full-length mutant construct SOE product. Mutant constructs were introduced into *V. cholerae* cells by chitin-induced natural transformation and/or cotransformation exactly as previously described (53, 54) or by chitin-independent transformations using a plasmid that ectopically expresses *tfoX* and *qstR* as previously described (55). For chitin-dependent natural transformation, *V. cholerae* was grown to mid-log in LB medium, washed with Instant Ocean medium (7 g/liter; Aquarium Systems), and incubated with chitin flakes (Alfa Aesar) at a final optical density at 600 nm (OD_{600}) of 0.1 overnight at 30°C. The next day, SOE PCR products were added to chitin-induced cells, incubated at 30°C for 5 h, and then outgrown and plated on selective media. For chitin-independent transformation, cells harboring pMMB67EH-*tfoX-qstR* were grown overnight in LB medium supplemented with 100 μM IPTG and 1 μg/ml chloramphenicol. The next day, 7 μl of the overnight culture was diluted into 350 μl of Instant Ocean medium. Then, SOE products were added as described above for chitin-dependent transformations. Mutant strains were confirmed by colony PCR, mismatch amplification mutation assay (MAMA) PCR (56), and/or sequencing. Complete lists of strains and primers used in this study are outlined in Table 2 and Table 1, respectively.

Measuring GFP and mCherry fluorescence in bulk populations. GFP and mCherry fluorescence in reporter strains were determined exactly as previously described (57). Briefly, single colonies were grown in LB overnight at 30°C. Where indicated, medium was supplemented with 10 μM CAI-1. CAI-1 was synthesized exactly as previously described (58). The next day, cells were washed and resuspended to an OD_{600} of 1.0 in Instant Ocean medium (7 g/liter; Aquarium Systems). Fluorescence was determined on a BioTek H1M plate reader. For GFP measurements, excitation was set to 500 nm and emission was set to 540 nm; for mCherry measurements, excitation was set to 580 nm and emission was set to 610 nm.

Antibody generation. Purified *Vibrio harveyi* LuxR protein (300 μg; purified as previously described [59]) was sent to Cocalico Biologicals, Inc. for serial injection into a rabbit host for antibody generation. Serum obtained from the third bleed has been used for Western analyses.

Western blotting. From overnight cultures, cells were concentrated to an OD_{600} of 20 in Instant Ocean medium. Cells were lysed on a FastPrep-24 classic instrument at 4°C, and then lysates were clarified by centrifugation. Lysates were then boiled with an equal volume of 2× SDS-PAGE sample buffer (220 mM Tris, pH 6.8, 25% glycerol, 1.2% SDS, 0.02% bromophenol blue, and 5% β-mercaptoethanol). Proteins were separated on a 15% SDS polyacrylamide gel by SDS electrophoresis, electrophoretically transferred to a polyvinylidene difluoride (PVDF) membrane, and probed with rabbit polyclonal α-LuxR serum or mouse monoclonal α-RpoA (BioLegend) primary antibodies. LuxR is the HapR homolog in *Vibrio harveyi* and has 72% identity and 86% similarity to *V. cholerae* HapR. The LuxR antibody was empirically found to be cross-reactive with *V. cholerae* HapR, and so it was used to detect HapR protein levels. Blots were then incubated with α-rabbit or α-mouse horseradish peroxidase (HRP)-conjugated secondary antibodies, developed using Pierce ECL Western blotting substrate (Thermo Fisher), and exposed to film.

Chitin bead culturing. Chitin beads (200 μl of a 50% slurry; NEB) and overnight cultures of the indicated strains were washed with defined artificial salt water (DASW) medium, which was prepared exactly as previously described (8). Chitin beads were inoculated with *V. cholerae* cells to an OD_{600} of 0.1 in a final volume of 5 ml in a Costar 6-well plate (Corning). Chitin mixtures were incubated statically at 30°C for 7 days before imaging.

Microscopy data collection and analysis. To image chitin beads, cultured beads were gently transferred to a coverslip using wide-bore pipette tips. To image chitin-grown cells, chitin bead reaction mixtures were vortexed and then centrifuged at 250 × *g* for 1 min. Cells found in the supernatant were transferred to a coverslip. To image Δ*cbp* strains, overnight cultures grown in LB were washed and resuspended to an OD_{600} of 0.2 in DASW and then transferred to a coverslip. Samples on the coverslip

TABLE 1 Primers used in this study

Primer	Sequence[a]	Description
Used for inverse PCR		
BBC 244	CCCGGGATCCTGTGTGAAATTGTTATCCGC	Tn*10*-specific primer for inverse PCR
BBC 434	GTGTGGGCACTCGACATATGACAAG	Tn*10*-specific primer for inverse PCR
Used for reporter constructs		
ABD 332	GGCTGAACGTGGTTGTCGAAAATGAC	Δ*lacZ* F1 (up arm)
BBC 219	GTTTATTTTTGTCGACTGTACAGCGTTTAAATAGAGGTCGATATTGACCC	Δ*lacZ* R1 (up arm)
ABD 342	ATTTTTCAGTTGGCCTACAATGCTTTCC	ΔVC1807 F1 (up arm)
BBC 719	CACCATACCCACGCCGAAACAAGGATTTTGAATTAAACGTTTCATTAGTC	ΔVC1807 R1 (up arm)
BBC 218	CGCTGTACAGTCGACAAAAATAAAC	Kan^r F (middle arm)
BBC 262	TACCGAGGACGCGAAGCTG	Kan^r R (middle arm)
BBC 266	CAGCTTCGCGTCCTCGGTAGAATAAAGCAATCCGCAAGCG	P_{chb} F (middle arm)
BBC 267	CCCGGGATCCTGTGTGAAATTGAGTTGCTTTCATTTCACTAATGG	P_{chb} R (middle arm)
BBC 732	ctcaagccgaggagtaaagaagAGTTGCTTTCATTTCACTAATGG	P_{chb} fuse to *lacZ* R (middle arm)
BBC 252	CAATTTCACACAGGATCCCGGGAGGAGGTAACGTAATGCGTAAAGGAGAAGAAC	GFP F (middle arm)
BBC 254	tgtaggctggagctgcttcTTAGTTGTATAGTTCATCCATGCC	GFP R (middle arm)
BBC 1356	TTGTTTCGGCGTGGGTATGGTGCGCTGTACAGTCGACAAAAATAAAC	mCherry F (middle arm)
BBC 206	tgtaggctggagctgcttcttacttgtacagctcgtccatg	mCherry R (middle arm)
ABD 785	CTTCTTTACTCCTCGGCTTGAG	P_{chb} stitch to *lacZ* F (down arm)
ABD 255	gaagcagctccagcctacaCCACAATAAGCCAGAGAGCCTTAAG	Δ*lacZ* F2 (down arm)
ABD 256	CCCAAATACGGCAACTTGGCG	Δ*lacZ* R2 (down arm)
ABD 341	gaagcagctccagcctacaTAGTCGAAAATAAAAAAAAGAGGCTCGCCTC	ΔVC1807 F2 (down arm)
ABD 345	CTTGCTAACCGTTGGTGTTACCAGC	ΔVC1807 R2 (down arm)
BBC 3083	tggataactttacgggcatgcataaggctcgtataatatattcagggagaccacaacggtttccctctac aaataattttgtttaactttCAATTTCACACAGGATCCCGGG	P_{const2} F
BBC 3082	ttatacgagccttatgcatgcccgtaaagttatccagcaaccactcatagacctagggcagcagatagg gacgacgtggtgttagctgtgCTCATTAGGCACCCCAGGC	P_{const2} R
Used for SOE deletion, FLAG fusions, and point mutants		
BBC 742	attccggggatccgtcgacCTGCAGTTCagaagcagctccagcctaca	MiniFRT F
BBC 743	tgtaggctggagctgcttctGAACTGCAGgtcgacggatccccggaat	MiniFRT R
ABD 123	ATTCCGGGGATCCGTCGAC	Kan^r, Spec^r, Carb^r, Cm^r, or Tm^r cassette F
ABD 124	TGTAGGCTGGAGCTGCTTC	Kan^r, Spec^r, Carb^r, Cm^r, or Tm^r cassette R
ABD 796	TTAGAATCTGCGCCAGAAGCG	Δ*cbp* F1 (up arm)
ABD 797	gtcgacggatccccggaatCATAGCTGTTCCTTACTAGTTGC	Δ*cbp* R1 (up arm)
BBC 920	gtcgacggatccccggaatGCTCATCAGGTCGTCAGCC	Δ3′ *cbp* R1 (up arm)
ABD 798	gaagcagctccagcctacaGTACTGGATCTGAAACCAGTTAAG	Δ*cbp* F2 (down arm)
ABD 799	GTATTGCGGAATGACCAGCATG	Δ*cbp* R2 (down arm)
BBC 2755	TTACCCCTAAGTCGGCGAGC	ΔVC0995 F1 (up arm)
BBC 2756	gtcgacggatccccggaatAATATTCACCTTAAGTTCCCCC	ΔVC0995 R1 (up arm)
BBC 2757	gaagcagctccagcctacaCTGCCTTAATCGAGTTTAAACCC	ΔVC0995 F2 (down arm)
BBC 2758	GCACCACGATAGCAATAAGC	ΔVC0995 R2 (down arm)
CAK 407	GCTACGCACTGCCAAATTACC	Δ*clpA* or Δ*clpS* F1 (up arm)
CAK 408	gtcgacggatccccggaatAAGCATAAGGCCTCCTTAAGGAAC	Δ*clpA* R1 (up arm)
CAK 409	gaagcagctccagcctacaCACTAGACATCTCACAATACGC	Δ*clpA* F2 (down arm)
CAK 410	CCGCTAACATCTCAGGACTG	Δ*clpA* or Δ*clpS* R2 (down arm)
CKP 449	TGCTCGGTTTTGATCCGTTC	Δ*clpP* or Δ*clpX* F1 (up arm)
CKP 450	gtcgacggatccccggaatGGGCGACATTGCATTTTTTTC	Δ*clpP* R1 (up arm)
CKP 451	gaagcagctccagcctacaGGCGAGTAAGCTCGTAATTG	Δ*clpP* F2 (down arm)
CKP 454	GTCAAACTAGAAACCAGCGC	Δ*clpP* or Δ*clpX* R2 (down arm)
CKP 447	gtcgacggatccccggaatTTTACTCATGACACTTCAATATTTG	Δ*clpS* R1 (up arm)
CKP 448	gaagcagctccagcctacaCAAGCTTAAACTTGCCGGGC	Δ*clpS* F2 (down arm)
CKP 452	gtcgacggatccccggaatGTCTGTCATTCGCTAACCTC	Δ*clpX* R1 (up arm)
CKP 453	gaagcagctccagcctacaGCGGAGTAATCTCAAGCAAC	Δ*clpX* F2 (down arm)
CKP 489	TTGACGCTCTGAAAGCAGAAG	Δ*lonA* F1 (up arm)
CKP 490	gtcgacggatccccggaatCAAGTTCATATTTTTCTCTCTTCCG	Δ*lonA* R1 (up arm)
CKP 491	gaagcagctccagcctacaGATGCATAGCAAAAATAAGTAAATC	Δ*lonA* F2 (down arm)
CKP 492	CGAAGAATTATAAGTGCAAAGGC	Δ*lonA* R2 (down arm)
BBC 422	ACGTTCAATAACCAGAATGTTGG	Δ*hapR* F1 (up arm)
BBC 423	gtcgacggatccccggaatTTTTCGATTGATGCGTCCATAG	Δ*hapR* R1 (up arm)
CKP 511	GTCtttgtcatcgtcatccttataatcCATAGGGGTATATCCTTGCC	1× FLAG-*hapR* R1 (up arm)
BBC 408	gaagcagctccagcctacaAACTAGTTTCTTGGGCAGCACAA	Δ*hapR* F2 (down arm)
CKP 510	ATGgattataaggatgacgatgacaaaGACGCATCAATCGAAAAACG	1× FLAG-*hapR* F2 (down arm)
BBC 409	GTTCATAATGATTTCCTTGGTGCC	Δ*hapR* R2 (down arm)
BBC 374	TGGCAAAAAGCGAGAGAAGAAG	Δ*luxO* F1 (up arm)

(Continued on next page)

TABLE 1 (Continued)

Primer	Sequence[a]	Description
BBC 375	gtcgacggatccccggaatCATGAGGACATATTTTGTTTTCTGC	Δ*luxO* R1 (up arm)
CKP 519	TCATATCTGGCAAACGTAAcTCCAGCAGGATTAAGTCAGG	*luxO*^{D47E} R1 (up arm)
BBC 376	gaagcagctccagcctacaTAAGCGATGAGAGAATGGATCAAC	Δ*luxO* F2 (down arm)
CKP 518	TGACTTAATCCTGCTGGAgTTACGTTTGCCAGATATGACG	*luxO*^{D47E} F2 (down arm)
BBC 377	TCACACCCGAATTTCCATCATGC	Δ*luxO* R2 (down arm)
CKP 554	GTCTCTTAGCCGAGGTACTG	Δ*cqsA* F1 (up arm)
CKP 555	gtcgacggatccccggaatCTTGTTCATCGCAATATATCCTAG	Δ*cqsA* R1 (up arm)
CKP 556	gaagcagctccagcctacaTTTCGTTAAATGCATAAATAACAAAAAC	Δ*cqsA* F2 (down arm)
CKP 557	AGTTGGAACCACTTCTTGTC	Δ*cqsA* R2 (down arm)
CKP 549	TACAACTGCTTGGCACGC	Δ*luxS* F1 (up arm)
CKP 550	gtcgacggatccccggaatTGGCATTTCCTTTCTCCC	Δ*luxS* R1 (up arm)
CKP 551	gaagcagctccagcctacaCACTAAGTCGGTTCTGTAAACG	Δ*luxS* F2 (down arm)
CKP 552	TTCTTAGCGTGATCAATTGC	Δ*luxS* R2 (down arm)
ABD 334	AGTGCTCCGGACTCTTTGCTCTG	Δ*lacZ* F1 (up arm)
ABD 254	gtcgacggatccccggaatCATCCCTCAAGCCGAGGAGTAAAG	Δ*lacZ* R1 (up arm)
ABD 255	gaagcagctccagcctacaCCACAATAAGCCAGAGAGCCTTAAG	Δ*lacZ* F2 (down arm)
ABD 256	CCCAAATACGGCAACTTGGCG	Δ*lacZ* R2 (down arm)
ABD 725	GAAGCAGCTCCAGCCTACA	Detect F for all deletions
BBC 082	gtcgacggatccccggaatCATAACTTACACCTTACTCACCCAG	Δ*cbp* detect R
CAK 411	TTGTTTGGTGCGATTATTGG	Δ*clpA* detect R
CKP 464	TTGGCAGAACATCTTTGATC	Δ*clpP* detect R
CKP 463	AAAGTATCCAGCTCACGGCG	Δ*clpS* detect R
CKP 465	CCATGTGTGGATAGACAACC	Δ*clpX* detect R
CKP 493	CAGTGCCACTTGGTCACCTG	Δ*lonA* detect R
BBC 410	TAAATGGGGCTTGGAGAATTTAG	Δ*hapR* detect R
BBC 1911	CGTAATCAAACTGCGAAAGTG	Δ*luxO* detect R
CKP 558	AATTCGTAACTCTGAGCATG	Δ*cqsA* detect R
CKP 553	TGGACCACGAACCTTAAACG	Δ*luxS* detect R
BBC 2759	TTGTCAGAAAGCGTTTCTGC	ΔVC0995 detect R
ABD 399	AACTGATGGCAGAAAAAGCCACTCAG	Δ*lacZ* detect R
BBC 993	ttgattataaggatgacgatgac	1× FLAG detect F
ABD 846	CATAAACATGTTTCTGATCAGCAG	1× FLAG-*hapR* detect R
BBC 380	GCCAATAGAATGAGTCTATTGGCTG	*luxO*^{D47E} detect F
CKP 520	TCATATCTGGCAAACGTAgc	*luxO*^{D47E} detect R
Used for EMSA probes		
BBC 744	cagcttcgcgtcctcggtaCGCAAATATAACTCAGGCAAAG	P_{chb} F
CKP 072	cccgggatcctgtgtgaaattgCTTTGGCAGGAGTAAGAAAACACCTAG	P_{chb} R
CKP 865	TAAGCAAACTGTAGCGTAGAAG	P_{clpP} F
CKP 866	TGCATTTTTTTCTTGGTAGC	P_{clpP} R
CKP 504	GCCAAATAAGTAAGTAAACACTAACAAACCTA	HapR BS 1 F
CKP 505	TAGGTTTGTTAGTGTTTACTTACTTATTTGGC	HapR BS 1 R
CKP 506	AATTGCAATTGATAAATTTCTTGGCTAGGTGT	HapR BS 2 F
CKP 507	ACACCTAGCCAAGAAATTTATCAATTGCAATT	HapR BS 2 R
Used for qPCR and qRT-PCR		
BBC 989	GCATCTAGGTTTTGACGTTTTTAACG	P_{chb} amplify F
BBC 990	AACACTCTCCAAGACCTACCTC	P_{chb} amplify R
ABD 132	CTGTCTCAAGCCGGTTACAA	*rpoB* amplify F
ABD 133	TTTCTACCAGTGCAGAGATGC	*rpoB* amplify R
CKP 865	TAAGCAAACTGTAGCGTAGAAG	P_{clpP} amplify F
CKP 867	TCGTATGAACGCTCACCACG	P_{clpP} amplify R
Used for purification vector		
JDN 92	agcagcggcctggtgccgcgcggcagcCatatggacgcatcaatcgaaaaa	Cloning 6×His-*hapR* into pET28b vector via IDA[b], F
JDN 93	tcagtggtggtggtggtggtgCTCGAGctagttcttatagatacacagcatattgagg	Cloning 6×His-*hapR* into pET28b vector via IDA, R
JDN 22	CTCGAGcaccaccaccacca	Amplify pET28b vector backbone for IDA, F
JDN 23	atGgctgccgcgcggcacca	Amplify pET28b vector backbone for IDA, R
Used for complementation constructs		
BBC 832	GCTTTTTGCTACAACGACCG	ΔVCA0692 F1 for up arm
BBC 828	CACCATACCCACGCCGAAACAACAGTGATGTAGCGAATCGGAC	ΔVCA0692 R1 for up arm
BBC 243	TTGTTTCGGCGTGGGTATGGTG	Tm^r or Zeo^r F for middle arm
BBC 647	tttttctatttctgaatcgattcatacgaCTCATTAGGCACCCCAGGC	Tm^r F or Zeo^r for middle arm
CKP 948	tcgtatgaatcgattcagaaatagaaaaaACCATTCTCGTTGTGTTGGG	P_{hapR}-*hapR* F for middle arm
BBC 729	tgtaggctggagctgcttcCTAGTTCTTATAGATACACAGCATATTG	P_{hapR}-*hapR* R for middle arm

(Continued on next page)

TABLE 1 (Continued)

Primer	Sequence[a]	Description
CKP 949	tcgtatgaatcgattcagaaatagaaaaaCCCTCATGCATTTTATAACTG	P_{clpSA}-*clpSA* F for middle arm
CKP 950	tgtaggctggagctgcttcCTAGTGGACCACCTCTTCGC	P_{clpSA}-*clpSA* R for middle arm
BBC 830	gaagcagctccagcctacaGTTGAGTTGGATGCAGCACC	ΔVCA0692 F2 for down arm
BBC 834	CACAATTTCTCGCTTAAAATGTCC	ΔVCA0692 R2 for down arm
CKP 509	gcaggtggagcaggtggaGACGCATCAATCGAAAAACG	ΔVCA0692::P_{hapR}-*hapR* detect F
BBC 1101	CAGACGTACTATTAACAGGACTGAC	ΔVCA0692::P_{hapR}-*hapR* detect R
CKP 235	gtcgacggatccccggaatCAAATATATCCTCCTCACTATTTTGATTAG	ΔVCA0692::P_{clpSA}-*clpSA* detect F
CKP 447	gtcgacggatccccggaatTTTACTCATGACACTTCAATATTTG	ΔVCA0692::P_{clpSA}-*clpSA* detect R

[a]Lowercase letters in primers indicate the sequence of overlap sequences needed for SOE PCR.
[b]IDA, isothermal DNA assembly.

were placed under a 0.2% Gelzan pad and imaged on an inverted Nikon Ti2 microscope with a Plan Apo 60× objective, yellow fluorescent protein (YFP) and mCherry filter cubes, a Hamamatsu ORCA-Flash 4.0 camera, and Nikon NIS-Elements imaging software.

The strains used to examine P_{chb} expression across a population contained (i) a P_{chb}-mCherry reporter and (ii) a reporter that drove constitutive expression of GFP, P_{const2}-GFP. By using these reporters, the expression of the P_{chb}-mCherry could be normalized to GFP expression in each cell. Images were analyzed on Fiji using the MicrobeJ plugin (60) to determine mean intensity of cells in the YFP and mCherry channels. GFP was assessed using a YFP filter set to avoid background fluorescence from chitin beads, which was stronger in the GFP channel. Background fluorescence was subtracted from each channel, and the mCherry/GFP fluorescence was determined for each individual cell.

HapR protein purification. A plasmid expressing a hexahistidine-tagged *hapR* wild-type (WT) allele was generated using Gibson assembly. The *hapR* insert was amplified from *V. cholerae* E7946 and inserted into a pET28b vector (Novagen) using the primers listed in Table 1. The plasmid was then electroporated into *E. coli* BL21(DE3) for protein overexpression. This strain was grown overnight in LB medium with kanamycin, back-diluted 1:100 into 1 liter of LB medium with kanamycin, and grown to an OD_{600} of 0.4 to 0.6 at 30°C. Expression of HapR was induced by IPTG to a final concentration of 1 mM, and cultures were grown for 4 h shaking at 30°C. The cells were pelleted and frozen at −80°C. The pellet was resuspended in 25 ml buffer A (25 mM Tris, pH 8, 500 mM NaCl), and an Avestin EmulsiFlex-C3 emulsifier was used to lyse cells. The soluble lysate was applied to a HisTrap HP nickel nitrilotriacetic acid (Ni-NTA) column using an Äkta Pure fast protein liquid chromatography (FPLC) system in buffer A and eluted from the column with a gradient of buffer B (25 mM Tris, pH 8, 500 mM NaCl, 1 M imidazole). The purified protein was concentrated to approximately 5 ml using Sartorius Vivaspin turbo 10,000 molecular weight cutoff (MWCO) centrifugal concentrators. The sample was manually injected into the Äkta Pure and separated via size exclusion chromatography on a HiLoad 16/600 Superdex 75-pg column equilibrated with gel filtration buffer (25 mM Tris, pH 7.5, 200 mM NaCl). Eluted fractions were analyzed by SDS-PAGE (15% gel), pooled, and concentrated using the same centrifugal concentrators previously mentioned. The samples were then immediately frozen in liquid nitrogen with a final concentration of 10% glycerol and stored at −80°C.

Electrophoretic mobility shift assay. Binding reactions contained 10 mM Tris HCl, pH 7.5, 1 mM EDTA, 10 mM KCl, 1 mM dithiothreitol (DTT), 50 μg/ml bovine serum albumin (BSA), 0.1 mg/ml salmon sperm DNA, 5% glycerol, 1 nM Cy5-labeled DNA probe, and HapR at the indicated concentrations (diluted in 10 mM Tris, pH 7.5, 10 mM KCl, 1 mM DTT, and 5% glycerol). Reaction mixtures were incubated at room temperature for 20 min in the dark and then electrophoretically separated on polyacrylamide gels in 0.5× Tris-borate-EDTA (TBE) buffer. Gels were imaged for Cy5 fluorescence on a Typhoon 9210 instrument. Short DNA probes (30 bp) were made by end-labeling one primer of a complementary pair (primers listed in Table 1) using 20 μM Cy5-dCTP and terminal deoxynucleotidyl transferase (TdT; Promega). Complementary primers (one labeled with Cy5 and the other unlabeled) were annealed by slow cooling at equimolar concentrations in annealing buffer (10 mM Tris, pH 7.5, and 50 mM NaCl). P_{chb} and P_{clpP} probes were made by Phusion PCR, where Cy5-dCTP was included in the reaction at a level that would result in incorporation of 1 to 2 Cy5-labeled nucleotides in the final probe as previously described.

ChIP-qPCR assays. Assays were carried out exactly as previously described (10). Briefly, overnight cultures were diluted to an OD_{600} of 0.08 and then grown for 6 h at 30°C. Cultures were cross-linked using 1% paraformaldehyde and then quenched with a 1.2 molar excess of Tris. Cells were washed with phosphate-buffered saline (PBS) and stored at −80°C overnight. The next day, cells were resuspended in lysis buffer (1× FastBreak cell lysis reagent [Promega], 50 μg/ml lysozyme, 1% Triton X-100, 1 mM phenylmethylsulfonyl fluoride [PMSF], and 1× protease inhibitor cocktail; 100× inhibitor cocktail contained the following: 0.07 mg/ml phosphoramidon [Santa Cruz], 0.006 mg/ml bestatin [MP Biomedicals/Fisher Scientific], 1.67 mg/ml AEBSF [4-(2-aminoethyl)benzenesulfonyl fluoride hydrochloride; DOT Scientific], 0.07 mg/ml pepstatin A [GoldBio], and 0.07 mg/ml E64 [Gold Bio]) and then lysed by sonication, resulting in a DNA shear size of ~500 bp. Lysates were incubated with anti-FLAG M2 magnetic beads (Sigma), washed to remove unbound proteins, and then bound protein-DNA complexes were eluted off with SDS. Samples were digested with proteinase K, then cross-links were reversed. DNA samples were cleaned up and used as a template for quantitative PCR (qPCR) using iTaq Universal SYBR green supermix (Bio-Rad) and primers specific for the genes indicated (primers are listed in Table 1) on a StepOne qPCR system. Standard curves of genomic DNA were included in each experiment and were used to determine the abundance of each amplicon in the input (derived from the lysate prior to ChIP) and output (derived

TABLE 2 Strains used in this study

Strain designation	Reference(s) in this report	Genotype	Reference
SAD 030	*V. cholerae* E7946 WT; parent for all other E7946 strains; Fig. S2 parent	*V. cholerae* E7946 O1 El Tor	50
SAD 2825	Activator screen strain	*V. cholerae* E7946 ΔVC1807::P_{chb}-mCherry, Kan^r; P_{chb}-*lacZ*, Spec^r; ΔVCA0692::*chiS*, Tm^r; Δ3′ *cbp*, pDL1086 Cm^r Carb^r	This study
SAD 2826	Δ*clpA* strain counterscreen	*V. cholerae* E7946 ΔVC1807::P_{chb}-mCherry, Kan^r; P_{chb}-*lacZ*, Spec^r; Δ*clpA*; Δ*cbp*::Tm^r; pDL1086, Cm^r Carb^r	This study
SAD 1309	Fig. 1 and 4 parent; Fig. S5 HapR WT	*V. cholerae* E7946 Δ*lacZ*::P_{chb}-GFP, Kan^r; Δ*cbp*::Spec^r	11
SAD 2827	Fig. 1 and 4 Δ*clpA* strain	*V. cholerae* E7946 Δ*lacZ*::P_{chb}-GFP, Kan^r; Δ*clpA*::Carb^r; Δ*cbp*::Spec^r	This study
SAD 2828	Fig. 1 Δ*clpP* strain	*V. cholerae* E7946 Δ*lacZ*::P_{chb}-GFP, Kan^r; Δ*clpP*::Carb^r; Δ*cbp*::Tm^r	This study
SAD 2829	Fig. 1 Δ*clpAP* strain	*V. cholerae* E7946 Δ*lacZ*::P_{chb}-GFP, Kan^r; Δ*clpA*::Carb^r; Δ*clpP*::Tm^r; Δ*cbp*::Spec^r	This study
SAD 2830	Fig. 1 Δ*clpS* strain	*V. cholerae* E7946 Δ*lacZ*::P_{chb}-GFP, Kan^r; Δ*clpS*::Carb^r; Δ*cbp*::Tm^r	This study
SAD 2831	Fig. 1 Δ*clpX* strain	*V. cholerae* E7946 Δ*lacZ*::P_{chb}-GFP, Kan^r; Δ*clpX*::Carb^r; Δ*cbp*::Tm^r	This study
SAD 2832	Fig. 1 Δ*lonA* strain	*V. cholerae* E7946 Δ*lacZ*::P_{chb}-GFP, Kan^r; Δ*lonA*::Tm^r; Δ*cbp*::Carb^r	This study
SAD 2833	Fig. 1 Δ*hapR* Δ*clpA* strain	*V. cholerae* E7946 Δ*lacZ*::P_{chb}-GFP, Kan^r; Δ*hapR*::Spec^r; Δ*clpA*::Carb^r; Δ*cbp*::Tm^r	This study
SAD 2834	Fig. 1 Δ*hapR* strain	*V. cholerae* E7946 Δ*lacZ*::P_{chb}-GFP, Kan^r; Δ*hapR*::Spec^r; Δ*cbp*::Carb^r	This study
SAD 2835	Fig. 2 parent	*V. cholerae* E7946 Δ*lacZ*::P_{chb}-mCherry, Kan^r; ΔVCA0692::P_{const2}-GFP, Spec^r	This study
SAD 2836	Fig. 2 Δ*hapR* strain	*V. cholerae* E7946 Δ*lacZ*::P_{chb}-mCherry, Kan^r; ΔVCA0692::P_{const2}-GFP, Spec^r; Δ*hapR*::Cm^r	This study
SAD 2837	Fig. 2 Δ*cbp* strain and Fig. S3 E7946 parent	*V. cholerae* E7946 Δ*lacZ*::P_{chb}-mCherry, Kan^r; ΔVCA0692::P_{const2}-GFP, Spec^r; Δ*cbp*::Tm^r	This study
SAD 2838	Fig. 2 Δ*hapR* Δ*cbp* strain and Fig. S3 E7946 Δ*hapR* strain	*V. cholerae* E7946 Δ*lacZ*::P_{chb}-mCherry, Kan^r; ΔVCA0692::P_{const2}-GFP, Spec^r; Δ*hapR*::Cm^r; Δ*cbp*::Tm^r	This study
SAD 2839	Fig. 3 ChIP strain and Fig. S5 1× FLAG-HapR	*V. cholerae* E7946 Δ*lacZ*::P_{chb}-GFP, Kan^r; 1× FLAG-*hapR*; Δ*cbp*::Tm^r	This study
SAD 2840	Fig. 4 Δ*luxO* strain	*V. cholerae* E7946 Δ*lacZ*::P_{chb}-GFP, Kan^r; Δ*luxO*::Spec^r; Δ*cbp*::Carb^r	This study
SAD 2841	Fig. 4 *luxO*^{D47E} strain	*V. cholerae* E7946 Δ*lacZ*::P_{chb}-GFP, Kan^r; *luxO*^{D47E}; Δ*cbp*::Spec^r	This study
SAD 2842	Fig. 4 Δ*luxS* strain	*V. cholerae* E7946 Δ*lacZ*::P_{chb}-GFP, Kan^r; Δ*luxS*::Cm^r; Δ*cbp*::Spec^r	This study
SAD 2843	Fig. 4 Δ*cqsA* strain	*V. cholerae* E7946 Δ*lacZ*::P_{chb}-GFP, Kan^r; Δ*cqsA*::Tm^r; Δ*cbp*::Spec^r	This study
SAD 2844	Fig. 4 Δ*cqsA* Δ*hapR* strain	*V. cholerae* E7946 Δ*lacZ*::P_{chb}-GFP, Kan^r; Δ*cqsA*::Tm^r; Δ*hapR*::Cm^r; Δ*cbp*::Spec^r	This study
SAD 306	*V. cholerae* A1552 WT; parent for all other A1552 strains	*V. cholerae* A1552 O1 El Tor	51
SAD 2908	*E. coli* strain used to mate pMMB tfoX-qstR into complementation strains used in Fig. S1	*E. coli* S17 harboring pMMB67EH *tfoX qstR*, Cm^r	This study
SAD 2909	Fig. S1 Δ*hapR* strain P_{hapR}-*hapR*	*V. cholerae* E7946 Δ*lacZ*::P_{chb}-GFP Kan^r; Δ*hapR*::Spec^r; Δ*cbp*::Carb^r; ΔVCA0692::P_{hapR}-*hapR*, Tm^r	This study
SAD 2910	Fig. S1 Δ*hapR* Δ*clpA* strain P_{hapR}-*hapR*	*V. cholerae* E7946 Δ*lacZ*::P_{chb}-GFP Kan^r; Δ*hapR*::Spec^r; Δ*clpA*::Carb^r; Δ*cbp*::Tm^r; ΔVCA0692::P_{hapR}-*hapR*, Zeo^r	This study
SAD 2911	Fig. S1 Δ*clpA* strain P_{clpSA}-*clpSA*	*V. cholerae* E7946 Δ*lacZ*::P_{chb}-GFP Kan^r; Δ*clpA*::Carb^r; Δ*cbp*::Spec^r; ΔVCA0692::P_{clpSA}-*clpSA*, Tm^r	This study
SAD 2912	Fig. S2 Δ*hapR* strain	*V. cholerae* E7946 Δ*hapR*::Cm^r	This study
SAD 2845	Fig. S3 A1552 parent	*V. cholerae* A1552 ΔVCA0692::P_{const2}-GFP, Spec^r; Δ*lacZ*::P_{chb}-mCherry, Kan^r; Δ*cbp*::Tm^r	This study
SAD 2846	Fig. S3 A1552 Δ*hapR* strain	*V. cholerae* A1552 ΔVCA0692::P_{const2}-GFP, Spec^r; Δ*lacZ*::P_{chb}-mCherry, Kan^r; Δ*hapR*::Cm^r; Δ*cbp*::Tm^r	This study
SAD 2847	Fig. S4 in WT *lacZ*$^+$ strain	*V. cholerae* E7946 ΔVC1807::Cm^r; ΔVC0995	This study
SAD 2848	Fig. S4 WT Δ*lacZ* strain	*V. cholerae* E7946 Δ*lacZ*::Spec^r; ΔVC1807::Cm^r; ΔVC0995	This study
SAD 2849	Fig. S4 Δ*hapR* Δ*lacZ* strain	*V. cholerae* E7946 Δ*lacZ*::Spec^r; ΔVC1807::Cm^r; ΔVC0995; Δ*hapR*::Tm^r	This study
JDN 71	Fig. 3B and C purified HapR	*E. coli* BL21(DE3) harboring pET28b-6×His-*hapR*, Kan^r	This study

from the samples after ChIP). Primers to amplify *rpoB* served as a baseline control in this assay because HapR does not bind this locus. Data are reported as "fold enrichment," which is defined as the ratio of the test promoter (P_{chb} or P_{clpP})/*rpoB* found in the output divided by the same ratio found in the input.

Chitobiose competition. Overnight cultures grown in LB were washed with M9 medium and mixed 1:1. For each growth reaction mixture, 10^2 cells of this mixture was added to M9 medium supplemented with 0.2% chitobiose and 10 μM synthetic CAI-1 and grown shaking at 30°C for 24 h. After 24 h, ~10^2 cells from this mixture was used to inoculate fresh growth reactions to achieve additional generations of growth on chitobiose. This was repeated a third time after another 24 h. CAI-1 was supplemented

throughout these experiments to ensure consistently high levels of HapR expression throughout transfer steps. After each 24-h growth period, the CFU per milliliter was determined for each strain in the mixture by dilution plating on LB agar supplemented with X-Gal. Competing strains were discerned by blue/white screening as one was a *lacZ*$^+$ strain and the other was a Δ*lacZ* strain. A *lacZ*$^+$ strain was competed against a Δ*lacZ* strain (parent-parent competition) or against a Δ*lacZ* Δ*hapR* strain (Δ*hapR* strain-parent competition). *V. cholerae* can grow on chitobiose through the activity of the following two sugar transporters: the GlcNAc phosphotransferase system (PTS) transporter (VC0995) or the chitobiose ABC transporter (VC0616-0620). Because we wanted to study the regulation of the transporter encoded within the *chb* locus, all strains for this assay had a deletion in VC0995 that renders growth on chitobiose dependent on the *chb* locus as previously described (11). Competitive indices were calculated as the CFU ratio of the Δ*lacZ* strain/*lacZ*$^+$ strain after growth for the indicated number of generations divided by the CFU ratio of the Δ*lacZ* strain/*lacZ*$^+$ strain in the initial inoculum.

Statistics. Statistical comparisons were determined using Student's *t* test or one-way analysis of variance (ANOVA) with Tukey's posttest using GraphPad Prism software.

SUPPLEMENTAL MATERIAL

Supplemental material is available online only.

SUPPLEMENTAL FILE 1, PDF file, 0.9 MB.

ACKNOWLEDGMENTS

We thank Ryan Chaparian for offering experimental advice, David Grainger for helpful discussions, and Wai-Leung Ng for providing synthetic CAI-1.

This work was supported by grant R35GM128674 from the National Institutes of Health to A.B.D. and grant R35GM124698 from the National Institutes of Health to J.C.V.K.

REFERENCES

1. Pruzzo C, Vezzulli L, Colwell RR. 2008. Global impact of *Vibrio cholerae* interactions with chitin. Environ Microbiol 10:1400–1410. https://doi.org/10.1111/j.1462-2920.2007.01559.x.
2. Huq A, Small EB, West PA, Huq MI, Rahman R, Colwell RR. 1983. Ecological relationships between *Vibrio cholerae* and planktonic crustacean copepods. Appl Environ Microbiol 45:275–283. https://doi.org/10.1128/AEM.45.1.275-283.1983.
3. Nahar S, Sultana M, Naser MN, Nair GB, Watanabe H, Ohnishi M, Yamamoto S, Endtz H, Cravioto A, Sack RB, Hasan NA, Sadique A, Huq A, Colwell RR, Alam M. 2011. Role of shrimp chitin in the ecology of toxigenic *Vibrio cholerae* and cholera transmission. Front Microbiol 2:260. https://doi.org/10.3389/fmicb.2011.00260.
4. Hunt DE, Gevers D, Vahora NM, Polz MF. 2008. Conservation of the chitin utilization pathway in the *Vibrionaceae*. Appl Environ Microbiol 74:44–51. https://doi.org/10.1128/AEM.01412-07.
5. Colwell RR, Huq A, Islam MS, Aziz KM, Yunus M, Khan NH, Mahmud A, Sack RB, Nair GB, Chakraborty J, Sack DA, Russek-Cohen E. 2003. Reduction of cholera in Bangladeshi villages by simple filtration. Proc Natl Acad Sci U S A 100:1051–1055. https://doi.org/10.1073/pnas.0237386100.
6. Huq A, Yunus M, Sohel SS, Bhuiya A, Emch M, Luby SP, Russek-Cohen E, Nair GB, Sack RB, Colwell RR. 2010. Simple sari cloth filtration of water is sustainable and continues to protect villagers from cholera in Matlab, Bangladesh. mBio 1:e00034-10. https://doi.org/10.1128/mBio.00034-10.
7. Meibom KL, Li XB, Nielsen AT, Wu CY, Roseman S, Schoolnik GK. 2004. The *Vibrio cholerae* chitin utilization program. Proc Natl Acad Sci U S A 101:2524–2529. https://doi.org/10.1073/pnas.0308707101.
8. Meibom KL, Blokesch M, Dolganov NA, Wu CY, Schoolnik GK. 2005. Chitin induces natural competence in *Vibrio cholerae*. Science 310:1824–1827. https://doi.org/10.1126/science.1120096.
9. Li X, Roseman S. 2004. The chitinolytic cascade in *Vibrios* is regulated by chitin oligosaccharides and a two-component chitin catabolic sensor/kinase. Proc Natl Acad Sci U S A 101:627–631. https://doi.org/10.1073/pnas.0307645100.
10. Klancher CA, Yamamoto S, Dalia TN, Dalia AB. 2020. ChiS is a noncanonical DNA-binding hybrid sensor kinase that directly regulates the chitin utilization program in *Vibrio cholerae*. bioRxiv https://doi.org/10.1101/2020.01.10.902320.
11. Klancher CA, Hayes CA, Dalia AB. 2017. The nucleoid occlusion protein SlmA is a direct transcriptional activator of chitobiose utilization in *Vibrio cholerae*. PLoS Genet 13:e1006877. https://doi.org/10.1371/journal.pgen.1006877.
12. Fuqua WC, Winans SC, Greenberg EP. 1994. Quorum sensing in bacteria: the LuxR-LuxI family of cell density-responsive transcriptional regulators. J Bacteriol 176:269–275. https://doi.org/10.1128/jb.176.2.269-275.1994.
13. Jung SA, Chapman CA, Ng WL. 2015. Quadruple quorum-sensing inputs control *Vibrio cholerae* virulence and maintain system robustness. PLoS Pathog 11:e1004837. https://doi.org/10.1371/journal.ppat.1004837.
14. Ball AS, Chaparian RR, van Kessel JC. 2017. Quorum sensing gene regulation by LuxR/HapR master regulators in vibrios. J Bacteriol 199:e00105-17. https://doi.org/10.1128/JB.00105-17.
15. Suckow G, Seitz P, Blokesch M. 2011. Quorum sensing contributes to natural transformation of *Vibrio cholerae* in a species-specific manner. J Bacteriol 193:4914–4924. https://doi.org/10.1128/JB.05396-11.
16. Sun S, Tay QX, Kjelleberg S, Rice SA, McDougald D. 2015. Quorum sensing-regulated chitin metabolism provides grazing resistance to *Vibrio cholerae* biofilms. ISME J 9:1812–1820. https://doi.org/10.1038/ismej.2014.265.
17. Yamamoto S, Mitobe J, Ishikawa T, Wai SN, Ohnishi M, Watanabe H, Izumiya H. 2014. Regulation of natural competence by the orphan two-component system sensor kinase ChiS involves a non-canonical transmembrane regulator in *Vibrio cholerae*. Mol Microbiol 91:326–347. https://doi.org/10.1111/mmi.12462.
18. Yamamoto S, Ohnishi M. 2017. Glucose-specific enzyme IIA of the phosphoenolpyruvate:carbohydrate phosphotransferase system modulates chitin signaling pathways in *Vibrio cholerae*. J Bacteriol 199:e00127-17. https://doi.org/10.1128/JB.00127-17.
19. Blokesch M. 2012. Chitin colonization, chitin degradation and chitin-induced natural competence of *Vibrio cholerae* are subject to catabolite repression. Environ Microbiol 14:1898–1912. https://doi.org/10.1111/j.1462-2920.2011.02689.x.
20. Sauer RT, Baker TA. 2011. AAA+ proteases: ATP-fueled machines of protein destruction. Annu Rev Biochem 80:587–612. https://doi.org/10.1146/annurev-biochem-060408-172623.
21. Lee KJ, Jung YC, Park SJ, Lee KH. 2018. Role of heat shock proteases in quorum-sensing-mediated regulation of biofilm formation by *Vibrio* species. mBio 9:e02086-17. https://doi.org/10.1128/mBio.02086-17.
22. Davis JH, Rubin AJ, Sauer RT. 2011. Design, construction and characterization of a set of insulated bacterial promoters. Nucleic Acids Res 39:1131–1141. https://doi.org/10.1093/nar/gkq810.
23. Lo Scrudato M, Blokesch M. 2012. The regulatory network of natural competence and transformation of *Vibrio cholerae*. PLoS Genet 8:e1002778. https://doi.org/10.1371/journal.pgen.1002778.

24. Zhu J, Mekalanos JJ. 2003. Quorum sensing-dependent biofilms enhance colonization in *Vibrio cholerae*. Dev Cell 5:647–656. https://doi.org/10.1016/s1534-5807(03)00295-8.
25. van Kessel JC, Ulrich LE, Zhulin IB, Bassler BL. 2013. Analysis of activator and repressor functions reveals the requirements for transcriptional control by LuxR, the master regulator of quorum sensing in *Vibrio harveyi*. mBio 4:e00378-13. https://doi.org/10.1128/mBio.00378-13.
26. Lee DH, Jeong HS, Jeong HG, Kim KM, Kim H, Choi SH. 2008. A consensus sequence for binding of SmcR, a *Vibrio vulnificus* LuxR homologue, and genome-wide identification of the SmcR regulon. J Biol Chem 283:23610–23618. https://doi.org/10.1074/jbc.M801480200.
27. Bailey TL, Boden M, Buske FA, Frith M, Grant CE, Clementi L, Ren J, Li WW, Noble WS. 2009. MEME suite: tools for motif discovery and searching. Nucleic Acids Res 37:W202–W208. https://doi.org/10.1093/nar/gkp335.
28. Chaparian RR, Tran MLN, Miller Conrad LC, Rusch DB, van Kessel JC. 2020. Global H-NS counter-silencing by LuxR activates quorum sensing gene expression. Nucleic Acids Res 48:171–183. https://doi.org/10.1093/nar/gkz1089.
29. Jobling MG, Holmes RK. 1997. Characterization of *hapR*, a positive regulator of the *Vibrio cholerae* HA/protease gene *hap*, and its identification as a functional homologue of the *Vibrio harveyi luxR* gene. Mol Microbiol 26:1023–1034. https://doi.org/10.1046/j.1365-2958.1997.6402011.x.
30. Freeman JA, Lilley BN, Bassler BL. 2000. A genetic analysis of the functions of LuxN: a two-component hybrid sensor kinase that regulates quorum sensing in *Vibrio harveyi*. Mol Microbiol 35:139–149. https://doi.org/10.1046/j.1365-2958.2000.01684.x.
31. Freeman JA, Bassler BL. 1999. Sequence and function of LuxU: a two-component phosphorelay protein that regulates quorum sensing in *Vibrio harveyi*. J Bacteriol 181:899–906. https://doi.org/10.1128/JB.181.3.899-906.1999.
32. Neiditch MB, Federle MJ, Miller ST, Bassler BL, Hughson FM. 2005. Regulation of LuxPQ receptor activity by the quorum-sensing signal autoinducer-2. Mol Cell 18:507–518. https://doi.org/10.1016/j.molcel.2005.04.020.
33. Tu KC, Bassler BL. 2007. Multiple small RNAs act additively to integrate sensory information and control quorum sensing in *Vibrio harveyi*. Genes Dev 21:221–233. https://doi.org/10.1101/gad.1502407.
34. Freeman JA, Bassler BL. 1999. A genetic analysis of the function of LuxO, a two-component response regulator involved in quorum sensing in *Vibrio harveyi*. Mol Microbiol 31:665–677. https://doi.org/10.1046/j.1365-2958.1999.01208.x.
35. Miller MB, Skorupski K, Lenz DH, Taylor RK, Bassler BL. 2002. Parallel quorum sensing systems converge to regulate virulence in *Vibrio cholerae*. Cell 110:303–314. https://doi.org/10.1016/s0092-8674(02)00829-2.
36. Surette MG, Miller MB, Bassler BL. 1999. Quorum sensing in *Escherichia coli*, *Salmonella* Typhimurium, and *Vibrio harveyi*: a new family of genes responsible for autoinducer production. Proc Natl Acad Sci U S A 96:1639–1644. https://doi.org/10.1073/pnas.96.4.1639.
37. Bridges AA, Bassler BL. 2019. The intragenus and interspecies quorum-sensing autoinducers exert distinct control over *Vibrio cholerae* biofilm formation and dispersal. PLoS Biol 17:e3000429. https://doi.org/10.1371/journal.pbio.3000429.
38. Hurley A, Bassler BL. 2017. Asymmetric regulation of quorum-sensing receptors drives autoinducer-specific gene expression programs in *Vibrio cholerae*. PLoS Genet 13:e1006826. https://doi.org/10.1371/journal.pgen.1006826.
39. Kroh HE, Simon LD. 1990. The ClpP component of Clp protease is the sigma 32-dependent heat shock protein F21.5. J Bacteriol 172:6026–6034. https://doi.org/10.1128/jb.172.10.6026-6034.1990.
40. Grossman AD, Erickson JW, Gross CA. 1984. The *htpR* gene product of *E. coli* is a sigma factor for heat-shock promoters. Cell 38:383–390. https://doi.org/10.1016/0092-8674(84)90493-8.
41. Katayama Y, Gottesman S, Pumphrey J, Rudikoff S, Clark WP, Maurizi MR. 1988. The two-component, ATP-dependent Clp protease of *Escherichia coli*. Purification, cloning, and mutational analysis of the ATP-binding component. J Biol Chem 263:15226–15236.
42. Gerth U, Kruger E, Derre I, Msadek T, Hecker M. 1998. Stress induction of the Bacillus subtilis *clpP* gene encoding a homologue of the proteolytic component of the Clp protease and the involvement of ClpP and ClpX in stress tolerance. Mol Microbiol 28:787–802. https://doi.org/10.1046/j.1365-2958.1998.00840.x.
43. Pennetzdorfer N, Lembke M, Pressler K, Matson JS, Reidl J, Schild S. 2019. Regulated proteolysis in *Vibrio cholerae* allowing rapid adaptation to stress conditions. Front Cell Infect Microbiol 9:214. https://doi.org/10.3389/fcimb.2019.00214.
44. Schild S, Tamayo R, Nelson EJ, Qadri F, Calderwood SB, Camilli A. 2007. Genes induced late in infection increase fitness of *Vibrio cholerae* after release into the environment. Cell Host Microbe 2:264–277. https://doi.org/10.1016/j.chom.2007.09.004.
45. Benitez JA, Spelbrink RG, Silva A, Phillips TE, Stanley CM, Boesman-Finkelstein M, Finkelstein RA. 1997. Adherence of *Vibrio cholerae* to cultured differentiated human intestinal cells: an *in vitro* colonization model. Infect Immun 65:3474–3477. https://doi.org/10.1128/IAI.65.8.3474-3477.1997.
46. Benitez JA, Silva AJ, Finkelstein RA. 2001. Environmental signals controlling production of hemagglutinin/protease in *Vibrio cholerae*. Infect Immun 69:6549–6553. https://doi.org/10.1128/IAI.69.10.6549-6553.2001.
47. Drescher K, Nadell CD, Stone HA, Wingreen NS, Bassler BL. 2014. Solutions to the public goods dilemma in bacterial biofilms. Curr Biol 24:50–55. https://doi.org/10.1016/j.cub.2013.10.030.
48. Hawver LA, Giulietti JM, Baleja JD, Ng WL. 2016. Quorum sensing coordinates cooperative expression of pyruvate metabolism genes to maintain a sustainable environment for population stability. mBio 7:e01863-16. https://doi.org/10.1128/mBio.01863-16.
49. McDonough E, Kamp H, Camilli A. 2016. *Vibrio cholerae* phosphatases required for the utilization of nucleotides and extracellular DNA as phosphate sources. Mol Microbiol 99:453–469. https://doi.org/10.1111/mmi.13128.
50. Miller VL, DiRita VJ, Mekalanos JJ. 1989. Identification of *toxS*, a regulatory gene whose product enhances *toxR*-mediated activation of the cholera toxin promoter. J Bacteriol 171:1288–1293. https://doi.org/10.1128/jb.171.3.1288-1293.1989.
51. Yildiz FH, Liu XS, Heydorn A, Schoolnik GK. 2004. Molecular analysis of rugosity in a *Vibrio cholerae* O1 El Tor phase variant. Mol Microbiol 53:497–515. https://doi.org/10.1111/j.1365-2958.2004.04154.x.
52. Dalia AB, Lazinski DW, Camilli A. 2013. Characterization of undermethylated sites in *Vibrio cholerae*. J Bacteriol 195:2389–2399. https://doi.org/10.1128/JB.02112-12.
53. Dalia AB, McDonough E, Camilli A. 2014. Multiplex genome editing by natural transformation. Proc Natl Acad Sci U S A 111:8937–8942. https://doi.org/10.1073/pnas.1406478111.
54. Dalia AB. 2018. Natural cotransformation and multiplex genome editing by natural transformation (MuGENT) of *Vibrio cholerae*. Methods Mol Biol 1839:53–64. https://doi.org/10.1007/978-1-4939-8685-9_6.
55. Simpson CA, Podicheti R, Rusch DB, Dalia AB, van Kessel JC. 2019. Diversity in natural transformation frequencies and regulation across *Vibrio* species. mBio 10:e02788-19. https://doi.org/10.1128/mBio.02788-19.
56. Cha RS, Zarbl H, Keohavong P, Thilly WG. 1992. Mismatch amplification mutation assay (MAMA): application to the c-H-ras gene. PCR Methods Appl 2:14–20. https://doi.org/10.1101/gr.2.1.14.
57. Dalia AB. 2016. RpoS is required for natural transformation of *Vibrio cholerae* through regulation of chitinases. Environ Microbiol 18:3758–3767. https://doi.org/10.1111/1462-2920.13302.
58. Ng WL, Perez LJ, Wei Y, Kraml C, Semmelhack MF, Bassler BL. 2011. Signal production and detection specificity in Vibrio CqsA/CqsS quorum-sensing systems. Mol Microbiol 79:1407–1417. https://doi.org/10.1111/j.1365-2958.2011.07548.x.
59. Chaparian RR, Olney SG, Hustmyer CM, Rowe-Magnus DA, van Kessel JC. 2016. Integration host factor and LuxR synergistically bind DNA to coactivate quorum-sensing genes in *Vibrio harveyi*. Mol Microbiol 101:823–840. https://doi.org/10.1111/mmi.13425.
60. Ducret A, Quardokus EM, Brun YV. 2016. MicrobeJ, a tool for high throughput bacterial cell detection and quantitative analysis. Nat Microbiol 1:16077. https://doi.org/10.1038/nmicrobiol.2016.77.